Wireless Strain Measurement Based on a Microstrip Patch Antenna

Song Guorong *, *Sun Tingting*, *Lü Yan*, *Yan Tianting*, *Wang Xuedong*, *He Cunfu*, *Wu Bin*

College of Mechanical Engineering and Applied Electronics Technology, Beijing University of Technology, Beijing 100124, P. R. China

(Received 13 October 2016; revised 5 July 2017; accepted 16 August 2017)

Abstract: Wireless interrogation of a rectangular microstrip patch antenna for strain measurement is investigated by simulations. To analyze the antenna performance, a microstrip line-feeding patch antenna at 10 GHz is designed. A patch antenna wirelessly fed by a horn is proposed to measure the strain. The direction information of strain detected by the patch antenna is also considered. The strain can be detected both in the width and length directions. It is shown that the strain can be measured wirelessly using a standard horn antenna. This kind of wireless strain-sensing technique offers significant potential for wireless structural health monitoring (SHM), especially for high-end equipment.

Key words: strain measurement; wireless interrogation; microstrip patch antenna; structural health monitoring (SHM)

CLC number: TP212.9 **Document code**: A **Article ID**: 1005-1120(2017)05-0477-10

0 Introduction

High-end equipment can be applied in aerospace, civil, and mechanical engineering structures operates in a harsh environment (high temperature, high pressure, etc.). During long-term service, load-bearing structures including the main supporting parts are inevitably damaged due to fatigue or corrosion. Damages such as cracks gradually expand and eventually lead to complete failure[1]. Consequently, structural health monitoring (SHM) has been proposed recently to detect damages in complex structures.

SHM is mainly about implementing sensors to evaluate damages. A typical SHM system consists of sensors, a network to transfer data, and a computer to analyze it. A variety of sensing technologies have been developed to advance SHM. Cracks originate from stress concentration, and can be predicted by local deformations. However, cracks form at points of material imperfection, which are commonly random. Therefore, monitoring stress and deformation in fragile areas can help to predict their occurrence. Therefore, strain sensors are among the most important SHM sensors.

Based on their interfacing methods, strain sensors can be classified as wired and wireless types. Typical wired sensors like metal-foil strain gauges or accelerometers are widely used in SHM. However, they need many coaxial cables to link the sensors to the data analyzer. According to Celebi, each sensing channel for a mid-rise building is expensive, and about half of the price is for installation of lengthy cables[2,3]. Therefore, wireless SHM sensors are proposed, using wireless transceivers to eliminate cables. In a wireless sensor network, the sensors themselves are not changed; they are typically still accelerometers and strain gauges, which are connected

* Corresponding author, E-mail address: grsong@bjut.edu.cn.

How to cite this article: Song Guorong, Sun Tingting, Lü Yan, et al. Wireless strain measurement based on a microstrip patch antenna[J]. Trans. Nanjing Univ. Aero. Astro., 2017,34(5):477-486.
http://dx.doi.org/10.16356/j.1005-1120.2017.05.477

to wireless nodes using short wires. Wireless strain sensors enable a dense sensor deployment, and easy installation and reconfiguration; they can be efficiently networked in applications where sensor wiring is not possible. Most wireless sensors have a dedicated internal power source, which constitutes a large part of their weight and limits the lifespan of wireless sensor nodes.

Passive wireless sensors eliminate the battery, thus extending their lifespan. Butler et al. first used induction coupling for power and data transmission[4]. In this type of passive wireless sensor, a parallel LC tank circuit is connected to a coil. The reader coil magnetically couples to the sensor coil to induce energy into the sensor circuit and perform the measurement. However, this magnetic coupling incurs high losses and has a short interrogation distance[5,6]. A novel lightweight, low-cost, wireless sensor with simple geometry and a long lifespan has been developed[7,8]. This SHM sensor utilizes a patch antenna to sense the strain and transmit the measurement data.

Jin et al. developed a wireless strain sensor that can be embedded or bonded in/on structures[9]. The resonant frequency of the patch antenna shifts when strain varies. The patch antenna in this sensor is connected to an exterior antenna to enable remote interrogation. Deshmukh et al. used a light-activated switch at the patch antenna sensor node as the sensor mechanism to detect strain wirelessly[10-12]. However, the sensor does not work in conditions of strong light intensity, e. g. in outdoor light. The antenna is simply glued to a metallic surface; when subjected to strain, it deforms and its resonant frequency shifts. Zhang et al. combined radio frequency identification(RFID) technology with patch antenna, and proposed a type of RFID tag antenna sensor which successfully applied in defect detection[13-15]. Based on the RFID technology, Yi et al. also designed a patch antenna sensor which enable to measure both strain and crack. However, the working frequency of the RFID chip ranges from 840 MHz to 960 MHz[16-18]. Strain sensitivity is therefore limited, because the resonant frequency dominates the strain sensitivity, as proved by previous researchers[19]. Daliri utilized a circular microstrip patch antenna for strain measurement in aluminum and composite materials[20,21]. Xu and Huang estimated the maximum interrogation distance of a wireless strain-measurement system to be 26 m, based on a transmission line model[22].

A new method to wirelessly detect the resonant frequency of patch antennas is proposed. A standard WR-90 horn antenna is used to read the resonant frequency of a patch antenna. The wireless measurement of strain is investigated using numerical simulations.

1 Theoretical Analysis

The frequency of an antenna is determined by its size, and the change in an antenna′s physical dimensions can cause a change in frequency. A patch antenna is characterized as carrier-conformal. Therefore, when the carrier sustains stress deformation, the dimensions of the patch antenna deform, causing the antenna frequency to change, as shown in Fig. 1. So, by measuring the frequency of the antenna, it is feasible to obtain the strain applied to the carrier.

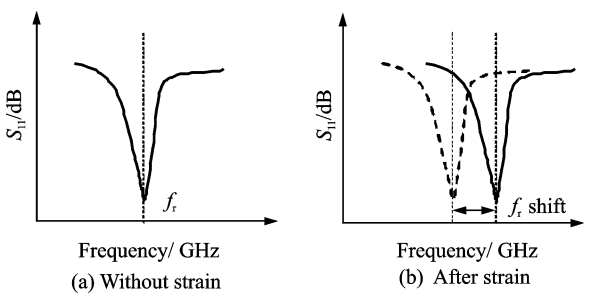

Fig. 1 Comparison of the patch antenna resonant frequency without strain and after strain

A typical rectangular microstrip patch antenna is shown in Fig. 2. The antenna consists of a very thin layer of copper as a patch, a layer of substrate and the ground plane. Among several analytical models for the patch antenna, the most simple and popular analytical model is transmission line model.

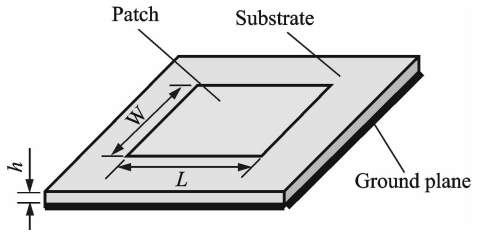

Fig. 2 Typical rectangular microstrip patch antenna

Based on the transmission line model, the resonant frequency f_r of a rectangular patch antenna can be calculated as

$$f_r = \frac{c}{2\sqrt{\varepsilon_{re}}} \frac{1}{L + 2\Delta L_{ex}} \tag{1}$$

where c is the velocity of light, ε_{re} the effective dielectric constant of the substrate, L the length of the antenna patch, and ΔL_{ex} the line extension. At the initial state, the antenna frequency f_{r0} is calculated from the antenna length L_0 and substrate thickness h_0.

After applying strain along the length direction, the patch length L will be stretched. Meanwhile, due to the influence of Poisson's ratio, the width of the patch W and the thickness of the dielectric substrate h will change to

$$W = (1 - \upsilon_P \varepsilon_L) W_0, \quad h = (1 - \upsilon_S \varepsilon_L) h_0 \tag{2}$$

Assuming that Poisson's ratio of the radiation patch and the dielectric substrate υ_P and υ_S are the same, we use υ to represent both. Then, the ratio W/h remains constant as the tensile strain ε_L changes. Therefore, the resonant frequency f_{r0} in Eq. (1) can be expressed as

$$f_{r0} = \frac{c}{2\sqrt{\varepsilon_{re}}} \frac{1}{L_0 + 2\Delta L_{oc}} = \frac{C_1}{L_0 + C_2 h_0} \tag{3}$$

where C_1 and C_2 can be calculated by

$$C_1 = \frac{c}{2\sqrt{\varepsilon_{re}}}$$

$$C_2 = \frac{0.812(\varepsilon_{re} + 0.3)(W_0/h_0 + 0.264)}{(\varepsilon_{re} - 0.258)(W_0/h_0 + 0.813)} \tag{4}$$

As a result, the strain-induced elongation will shift the antenna resonant frequency f_r. When the strain ε_L is applied, the resonant frequency shifts to

$$f_r(\varepsilon_L) = \frac{C_1}{L_0(1 + \varepsilon_L) + C_2 h_0 (1 - \upsilon \varepsilon_L)} \tag{5}$$

Finally, according to Eqs. (4) and (5), the relationship between the strain and the frequency shift can be established as

$$\varepsilon_L = -\frac{L_0 + \upsilon C_2 h_0}{L_0 + C_2 h_0} \frac{\Delta f}{f_{r0}} \tag{6}$$

where $\Delta f = f_r - f_{r0}$.

The strain can be measured by monitoring the resonant frequency of the patch antenna using the scattering parameter S_{11}, which indicates the amount of power that is "lost to the load" and does not return as a reflection. The frequency that corresponds to the minimum value of the S_{11} curve is the resonant frequency of the antenna.

Horn antennas are used to propagate a microwave into space, or to receive microwaves for reception devices. A typical rectangular horn antenna, shown in Fig. 3, consists of a rectangular waveguide, of which one side is closed, while the other side flares into an open-ended, and pyramid- shaped horn. In the diagram, E and H represent the direction of the electrical field and magnetic field, respectively.

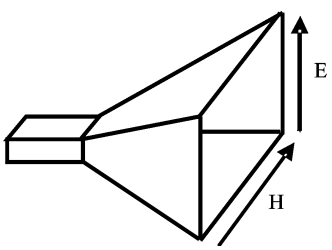

Fig. 3 Rectangular horn antenna model

When the horn radiates microwaves toward a rectangular patch antenna, the wave will transmit through the air to the patch, on which it forms an electric field. Resonance will occur if the length of the patch is slightly less than half the wavelength.

A rectangular patch antenna usually has two fundamental radiation modes: TM_{01} and TM_{10}. The TM_{10} mode indicates that the electric field varies half-wave along the patch antenna length direction, with no variation along the width direction, while the TM_{01} mode has electric field variation along the patch antenna's width direction and no variation along the length direction. Each radiation mode corresponds to a resonant frequency, thus two resonant frequencies shown in Fig. 4, denoted as f_{01} and f_{10}, can be detected respec-

tively by aligning the electric field polarization of the interrogating signal to be parallel to the polarization direction of a particular radiation mode. A resonant frequency can be detected by two orthogonal directions: One is parallel to the geometric length of the patch; and the other is parallel to its geometric width.

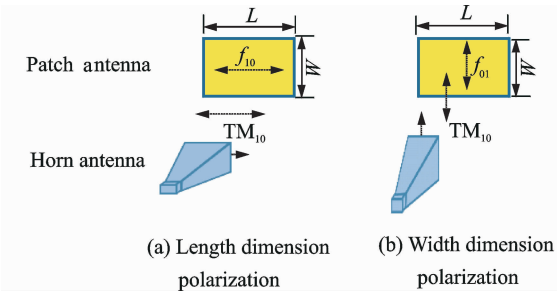

Fig. 4 Remote interrogation of the patch antenna

The horn radiates linearly-polarized radio waves toward the rectangular patch antenna, whose polarization direction is parallel to the patch antenna's geometric length, and the TM_{10} mode is polarized along the length direction, as shown in Fig. 4(a). Rotating the horn antenna by 90° will rotate the electric field polarization parallel to the patch antenna's geometric width, thus the TM_{01} mode is polarized along the length direction as shown in Fig. 4(b). In conclusion, strains can be wirelessly interrogated by a horn antenna in two directions, which are parallel to the geometric length and width of the patch.

2 Simulation Model

Here HFSS™ (High frequency structure simulator) is used to simulate the system for wireless interrogation of the patch antenna. HFSS™ software is a commercial finite element analysis (FEA) solver for electromagnetic structures. It is a popular application for complex radio frequency (RF) electromagnetic circuit design like antennas, filters, amplifiers, and transmission lines. It reduces the costs of experiments by simulating the actual conditions of an antenna under stress. For patch antennas, it provides a variety of antenna parameters, including S parameters, directivity, and far-field 3-D radiation patterns.

A radiation boundary allows waves to radiate infinitely far into space, e. g. for antenna design. HFSS absorbs the wave at the radiation boundary, essentially ballooning the boundary infinitely far from the structure. Air box shown in Fig. 5(a) is assigned radiation boundary, thus can be treated as an infinite large space. The patch and ground plane both are assigned perfect E boundaries, which represent perfectly conducting surfaces in a structure. To obtain the resonant frequency shift, a very fine mesh and very strict settings should be used in HFSS.

2.1 Antenna design

The dimensions of the patch antenna are initially set to the values calculated using a transmission model for a frequency of 10 GHz. Table 1 shows the patch antenna structure parameters given by theory[23]. According to Eq. (1), the patch geometric length directly affects the resonant frequency.

Table 1 Patch antenna structure parameter table

Parameter	L/mm	W/mm	h/mm
Patch	40	30	0
Substrate	120	90	1.6
Feed line	70	4.95	0
Ground plane	120	90	1.6
Air box	120	90	43.2

The substrate material is Rogers 5880, a type of glass microfiber-reinforced composite with dielectric permittivity of 2.2. The dielectric permittivity ε_r is the capacitance ratio between electrodes charged with a substance and the vacuum vessel, indicating the energy-storage capacity of a material, which is proportional to the dielectric loss. When ε_r is large, the storage-power capacity and energy loss are large. Therefore, in high-frequency transmission, the dielectric permittivity is required to be low. Rogers 5880 is chosen for its low dielectric permittivity.

The patch and ground plane both are assigned perfect E boundaries, which represent perfectly conducting surfaces in a structure. All the 3-D models mentioned below are created and simulated using HFSS.

To study the patch antenna performance, a microstrip line feeding patch antenna is first designed. A simulation model is described in Fig. 5(a). A 50-ohm lumped port emits microwaves to the patch antenna through a 50-ohm microstrip line and a 1/4λ-impedance transformer. A 1/4λ-impedance transformer is used to match the microstrip line impedance with the impedance of the patch. The top view of the model and the electric field distribution on the patch are shown in Fig. 5(b). There is electric field variation along the patch antenna width direction and no variation along the length direction, indicating that only the dominant mode TM_{01} is excited.

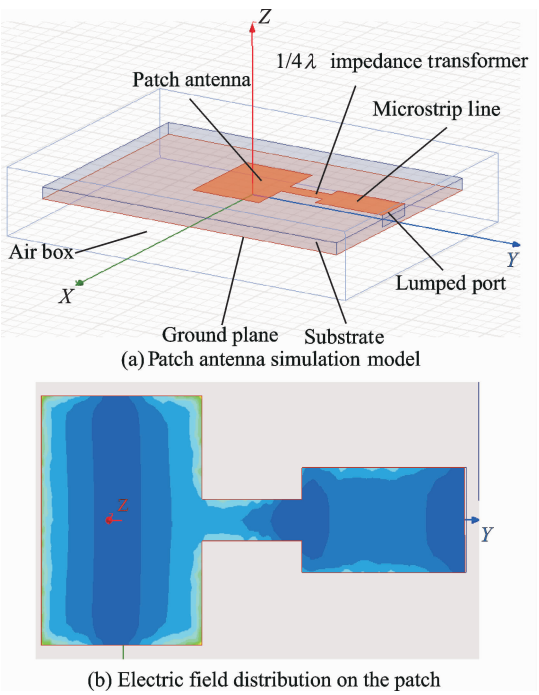

Fig. 5 Microstrip line-feeding patch antenna model and E field distribution

Simulated radiation patterns are obtained by far-field calculations in HFSS, as shown in Fig. 6. The radiation pattern in Fig. 6(a) shows that the peak gain is above the patch, therefore, the antenna reader used in wireless measurement is placed right above the patch. The radiation pattern in two planes in Fig. 6(b) shows the low side lobe and wide width of the main lobe, indicating the unfocused energy radiation. From the simulated S_{11} curve shown in Fig. 7, the simulated resonant frequency is 9.89 GHz, which agrees with the theoretical value of 10 GHz. For the purpose of wireless interrogation, the patch antenna must be excited using the electromagnetic wave emitted from a horn antenna. In this paper, a WR-90 standard-gain horn antenna is selected as the reader; this is a standard device for measuring antenna characteristics. The operating frequency bands of the WR-90 standard-gain horn antenna are 8.2—12.4 GHz, which contain the patch antenna's frequency.

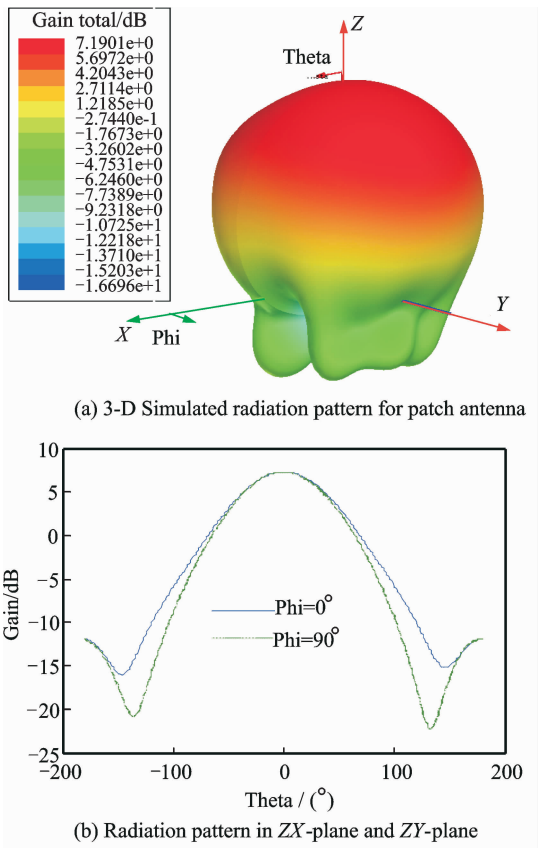

Fig. 6 Simulated radiation pattern of microstrip line-feeding patch antenna

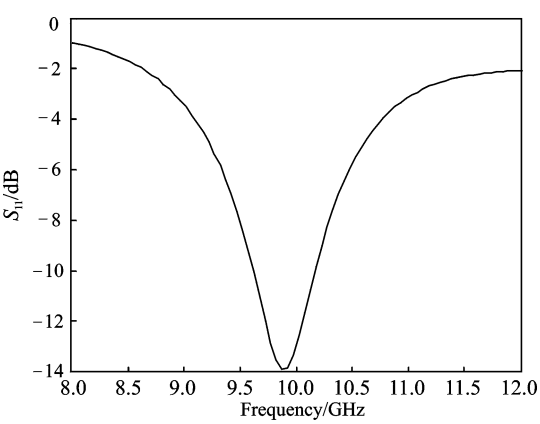

Fig. 7 Simulated S_{11} curve of patch antenna

2.2 Wireless interrogation model

To investigate the possibility of wireless interrogation of a patch antenna resonant frequency as well as the wireless strain measurement using a standard horn antenna, a patch antenna and a standard horn antenna are simulated using the HFSS electromagnetic software. Using HFSS, the lumped port is applied as the excitation source, and perfectly matched layers (PMLs) are used as absorbing boundary conditions.

The S_{11} curves of the horn antenna under four different scenarios are considered: A horn antenna only, an aluminum plate in front of the horn, an aluminum plate with a layer of substrate (Rogers 5880) on top and in front of the horn, and a patch antenna in front of the horn.

Fig. 8 shows the 3-D simulation model including the horn antenna model, patch antenna model, and boundary conditions.

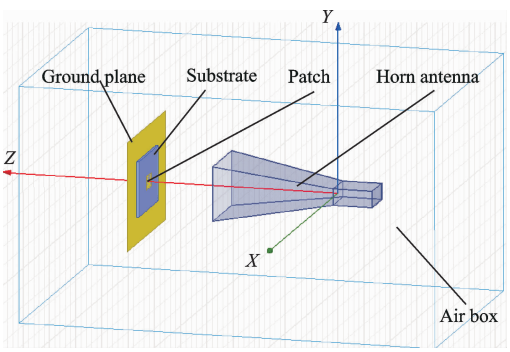

Fig. 8 Wireless interrogation of patch antenna

Fig. 9 shows the S_{11} scattering parameter of the horn antenna for the four scenarios discussed above at the frequency range from 8 GHz to 12 GHz. It is obvious that compared with nothing in front of the horn, the magnitude of S_{11} increases after adding the aluminum plate. This is because some energy reflects from the aluminum plate back into the horn, which can be interpreted as an increase in the reflected power at the port of the horn, thus leading to the increase in S_{11}. When a substrate is added on top of the plate, the level of the reflected power is slightly lower compared with the previous case due to the attenuation in the dielectric material, which explains why the magnitude of S_{11} decreases slightly.

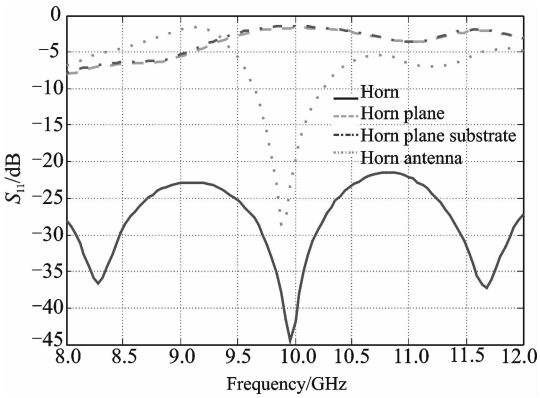

Fig. 9 Comparison of S_{11} in different scenarios

By adding the patch on top of the substrate (forming the patch antenna), the resonance occurs, and a dip is observed in the S_{11} curve at 9.89 GHz, which corresponds to the reference value measured by the microstrip line feeding the patch antenna. This indicates that the patch antenna's resonant frequency can be monitored using a horn antenna. Moreover, the conductive structure (ground plane) and the substrate do not disturb the wireless excitation of the patch.

3 Design and Simulation

For simulating the effect of the tensile strain along the width direction, the dimensions of the patch antenna under strain are calculated by Eq. (2). In this case, the horn antenna is polarized in the width dimension, and the TM_{01} mode is excited, where f_{01} is the resonant frequency. Table 2 shows the dimensions of the patch antenna under different strain levels ranging from 0% to 0.6%. In the simulation model, the excitation frequency is swept from 9.5 GHz to 10.1 GHz in steps of 0.001 GHz. This frequency band is chosen because the change in the length affects the frequency f_{01} only, which is 10 GHz.

Fig. 10 shows the simulated S_{11} curves of the patch antenna under tensile strains ranging from 0% to 0.6%. The frequency with the minimum value of the S_{11} curves corresponds to the resonant frequency. The minimum value of all seven S_{11} curves is below −30 dBm, which meets the standard (below −10 dBm). Simulation results show a continuous shift in the resonant frequency

of the patch antenna. As the applied tensile strain increases, the length of the patch increases, thus the S_{11} curve shifts to the left side, corresponding to a resonant frequency decrease.

Table 2 Patch antenna dimensions at different strains in length direction

Strain/%	h/mm	W/mm	L/mm
0	1.575	9.000	11.900
0.1	1.572	9.045	11.882
0.2	1.570	9.090	11.864
0.3	1.568	9.135	11.846
0.4	1.565	9.180	11.829
0.5	1.563	9.225	11.811
0.6	1.561	9.270	11.793

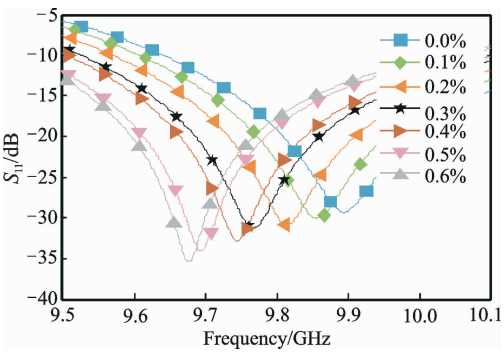

Fig. 10 Simulated S_{11} curves of patch antenna under strains along width direction

Fig. 11 shows the relationship between the resonant frequency f_{01} and the applied strain along the width direction. The slope of the linear fit represents the strain sensitivity of the sensor. In this case, the simulated strain sensitivity of the antenna sensor is 0.074 07, which corresponds to 74.07 kHz/$\mu\varepsilon$. The theoretical strain sensitivity of the antenna sensor is 78.56 kHz/$\mu\varepsilon$. Thus, the simulated and theoretical values agree. Based on the simulation results, it is feasible to wirelessly measure tensile strain when strain is applied along the geometric width of the patch.

The rectangular patch antenna has the other resonant mode TM_{10}, which has been studied in the same way. According to Eq. (1), the theoretical value of f_{10} is 7.94 GHz, which means a WR-90 horn (operating frequency bands 8.2—12.4 GHz) does not meet that requirement. Thus, we substitute a WR-112 horn, with operating frequency bands 7.0—10.0 GHz, for the WR-90 in the simulation model.

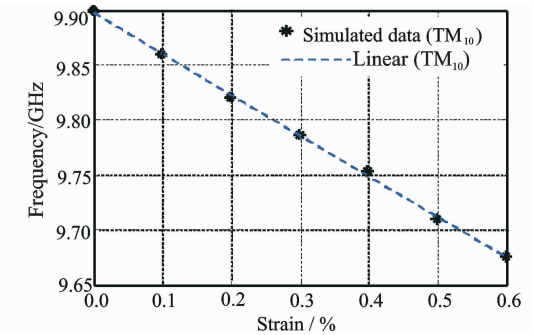

Fig. 11 Relationship between the resonant frequency and strain along width direction

In this case, the horn is polarized in the length dimension, and the TM_{10} mode is excited, where f_{10} is the resonant frequency. To simulate the effect of the tensile strain along the length direction, the dimensions of the patch antenna under strain are calculated by Eq. (2). Table 3 shows the dimensions of the patch antenna under different strain levels ranging from 7.6 GHz to 8.2 GHz in steps of 0.001 GHz. This frequency band is chosen because the change in length only affects the frequency f_{01}, which is 7.9 GHz.

Table 3 Patch antenna dimensions at different strains in length direction

Strain/%	H /mm	W/mm	L/mm
0	1.575	9.000	11.900
0.1	1.572	8.997	11.911
0.2	1.570	8.994	11.924
0.3	1.568	8.992	11.936
0.4	1.565	8.989	11.948
0.5	1.563	8.987	11.960
0.6	1.561	8.984	11.971

Fig. 12 shows the simulated S_{11} curves of the patch antenna under tensile strains ranging from 0% to 0.6%. Simulation results show a continuous shift in the resonant frequency of the patch antenna. As the applied tensile strain increases, the length of the patch increases, thus the S_{11} curve shifts to the left side, which means the res-

onant frequency decreases.

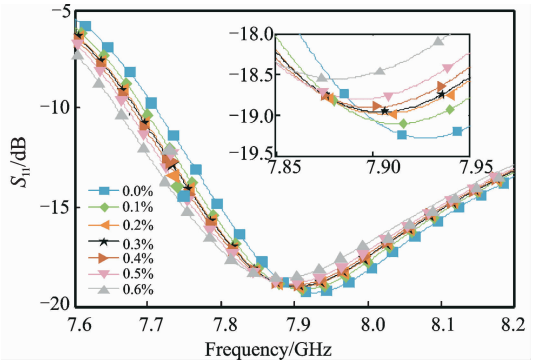

Fig. 12 Simulated S_{11} curves of patch antenna under strains along length direction

Fig. 13 shows the relationship between the resonant frequency f_{10} and the applied strain along the length direction. In this case, each S_{11} curve's minimum value is below −15 dBm, which meets the standard (below −10 dBm). The simulated strain sensitivity of the antenna sensor is 65.04 kHz/$\mu\varepsilon$, which is in accord with the theoretical value (66.98 kHz/$\mu\varepsilon$). Based on the simulation results, it is feasible to wirelessly measure tensile strain when strain is applied along the geometric length of the patch.

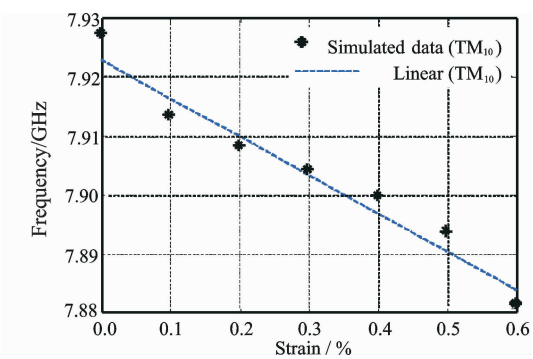

Fig. 13 Relationship between the resonant frequency and strain along length direction

Simulation results verify that a patch antenna can be wirelessly interrogated by a polarized rectangular horn. Both TM_{01} and TM_{10} of the rectangular patch antenna can be detected wirelessly. However, the minimum value of S_{11} curves of the TM_{01} mode is below −30 dBm, while corresponding value of the TM_{10} mode is only below −15 dBm. In addition, TM_{01} has much better linearity than TM_{10}. The linear correlation coefficients of TM_{01} and TM_{10} are 0.990 6 and 0.934 4, respectively. The sensitivity of TM_{01} is 74.07 kHz/$\mu\varepsilon$, while that of TM_{10} is 65.04 kHz/$\mu\varepsilon$. Thus, TM_{01} has 14% higher sensitivity than TM_{10}. Apparently, both modes can detect strain effectively. In summary, the TM_{01} mode shows better performance than the TM_{10} mode.

4 Conclusions

An innovative wireless strain measurement technique using a rectangular patch antenna sensor is investigated. Microstrip patch antennas are designed based on the transmission line model. Simulations using HFSS software are conducted to analyze the resonant frequency of the microstrip patch antenna sensors, by which the mechanical and electrical parameters of the antenna sensor can be manipulated. In simulations, the resonant frequency of the patch antenna can be achieved wirelessly by measuring the S_{11} parameter by a standard horn antenna.

A rectangular patch antenna generally possesses two fundamental radiation modes: TM_{01} and TM_{10}. Radiation modes can be switched by rotating the horn antenna. However, the minima of the TM_{01} mode in S_{11} curves are lower than those of the TM_{10} mode. Not only is the sensitivity of TM_{01} 14% higher than that of TM_{10}, the linearity of TM_{01} is much better as well. In summary, the TM_{01} mode shows better performance than the TM_{10} mode. Thus, strain can be detected in both the width and length directions of the patch.

The simulation results demonstrate that a rectangular patch antenna can be used for wireless strain measurement. Wireless monitoring of the shift in the resonant frequency of the patch antenna allows the strain applied in the host structure (ground plane) to be detected. However, the interrogation distance is limited, thus future work will be focused on increasing the interrogation distance and other experimental investigations.

Acknowledgments

This work was supported by the National Natural Science Foundation of China (Nos. 51575015,51235001,51505013).

References:

[1] HOU Bo, HE Yuting, GAO Chao, et al. Film sensor design for metallic structure crack monitoring [J]. Journal of Nanjing University of Aeronautics & Astronautics, 2014, 46(3): 419-424. (in Chinese)

[2] LIU Rongmei, XIAO Jun, LIANG Dakai, et al. Performance improvement method of CFRP with embedded optical fiber[J]. Transactions of Nanjing University of Aeronautics & Astronautics, 2015, 32(3): 261-267.

[3] CELEBI M, NISHENKO S P, ASTILL C, et al. Seismic instrumentation of federal buildings: A proposal document for consideration by federal agencies [R]. Washington DC: US Geological Survey, 1998: 98-117.

[4] BUTLER J C, VIGLIOTTI A J, VERDI F W, et al. Wireless, passive, resonant-circuit, inductively coupled, inductive strain sensor [J]. Sensors and Actuators A: Physical, 2002, 102(1): 61-66.

[5] GOULD D, MEINERS M, BENECKE W, et al. Condensation detection using a wirelessly powered RF-temperature sensor [J]. IEEE Transactions on Vehicular Technology, 2009, 58(4): 1667-1672.

[6] HARPSTER T J, STARK B, NAJAFI K. A passive wireless integrated humidity sensor [J]. Sensors and Actuators A: Physical, 2002, 95(2): 100-107.

[7] TATA U S. Study of patch antennas for strain measurement [D]. Arlington: The University of Texas at Arlington, 2008.

[8] TATA U, HUANG H, CARTER R L, et al. Exploiting a patch antenna for strain measurements [J]. Measurement Science and Technology, 2008, 20(1): 1-9.

[9] JIN X. Embedded antennas in concrete for application in wireless sensors [D]. Columbia: University of South Carolina, 2011.

[10] DESHMUKH S. Passive RF sensors and wireless sensor interrogation [D]. Arlington: The University of Texas at Arlington, 2010.

[11] DESHMUKH S, HUANG H. Wireless interrogation of passive antenna sensors [J]. Measurement Science and Technology, 2010, 21(3): 035201-035209.

[12] DESHMUKH S, MOHAMMAD I, XU X, et al. Unpowered antenna sensor for crack detection and measurement[J]. Proceedings of SPIE—The International Society for Optical Engineering, 2010, 7647 (764742): 1-9.

[13] ZHANG J, TIAN G Y. UHF RFID tag antenna-based sensing for corrosion detection & characterization using principal component analysis [J]. IEEE Transactions on Antennas & Propagation, 2016, 64 (10): 4405-4414.

[14] ZHANG J, TIAN G Y, MARINDRA A M J, et al. A review of passive RFID tag antenna-based sensors and systems for structural health monitoring applications [J]. Sensors, 2017, 17(2): 265-298.

[15] ZHANG J, TIAN G Y, ZHAO A B. Passive RFID sensor systems for crack detection & characterization [J]. NDT & E International, 2017, 86: 89-99.

[16] YI X, WU T, WANG Y, et al. Passive wireless smart-skin sensor using RFID-based folded patch antennas[J]. International Journal of Smart and Nano Materials, 2011, 2(1): 22-38.

[17] CHO C, YI X, WANG Y, et al. Compressive strain measurement using RFID patch antenna sensors [C]//SPIE Smart Structures and Materials+ Nondestructive Evaluation and Health Monitoring. San Diego: International Society for Optics and Photonics. 2014: 90610X-1-90610X-11.

[18] YI X, WU T, WANG Y, et al. Sensitivity modeling of an RFID-based strain-sensing antenna with dielectric constant change [J]. IEEE Sensors Journal, 2015, 15(11): 6147-6155.

[19] GE H Y, LI H, CHENG Y L, et al. A strain measurement method based on micro-strip patch antennas [J]. SCIENTIA SINICA Technologica, 2014, 44 (9): 973-978.

[20] DALIRI A, JOHN S, GALEHDAR A, et al. Strain measurement in composite materials using microstrip patch antennas[C]//ASME 2010 Conference on Smart Materials, Adaptive Structures and Intelligent Systems. Philadelphia: American Society of Mechanical Engineers, 2010: 591-598.

[21] DALIRI A, GALEHDAR A, ROWE W S T, et al. Utilizing micro-strip patch antenna strain sensors for structural health monitoring[J]. Journal of Intelligent Material Systems and Structures, 2012, 23(2):

169-182.

[22] XU X, HUANG H. Battery-less wireless interrogation of micro-strip patch antenna for strain sensing [J]. Smart Materials and Structures, 2012, 21(12): 1-7.

[23] BALANIS C A. Antenna theory: Analysis and design [M]. Hoboken: Harper & Row, 1982.

Prof. **Song Guorong** received her B. S. and Ph. D. degrees in 1986 and 2009 from Beijing University of Technology. She is currently a professor in Beijing University of Technology. Her main research interests include intelligent and virtual instruments, computer testing and control technology, sensors and precision measurement, nondestructive testing of new technologies, structural health monitoring, passive wireless strain sensing, and sensor design optimization.

Ms. **Sun Tingting** received her B. S. degree in 2010 from Lanzhou University of Technology. Now she is a postgraduate in Beijing University of Technology. Her main research interests include microwave nondestructive technique, structural health monitoring, passive wireless strain sensing, and sensor design optimization.

Dr. **Lü Yan** received his B. S. degree in 2008 from Beijing University of Aeronautics and Astronautics, Ph. D. degree in 2014 from Beijing University of Technology. Now he is a lecturer in Beijing University of Technology. His main research interests include acoustic microscopy technique, nondestructive testing of material mechanical properties and novel piezoelectric transducer.

Ms. **Yan Tianting** received her B. S. and M. S. degrees in 2011 and 2017 from Beijing University of Technology. Her main research interests include microwave nondestructive technique, structural health monitoring, passive wireless strain sensing.

Mr. **Wang Xuedong** received his B. S. degree in 2014 from Weifang University. Now he is a postgraduate in Beijing University of Technology. His main research interests include microwave nondestructive technique, structural health monitoring, passive wireless strain sensing, and sensor design optimization.

Prof. **He Cunfu** received his B. S., M. S. and Ph. D. degrees in 1985, 1990 and 1996 from Taiyuan University of Technology, Huazhong University of Science and Technology and Tsinghua University, respectively. He is currently a professor in Beijing University of Technology. His main research interests include mechanical testing theory method and technology, ultrasonic nondestructive testing technology, and sensor technology.

Prof. **Wu Bin** received his B. S., M. S. and Ph. D. degrees in 1984, 1990 and 1996 from Tianjin University, Beijing University of Aeronautics and Astronautics and Taiyuan University of Technology, respectively. He is currently a professor in Beijing University of Technology. His main research interests include experimental solid mechanics, modern measurement and control technology, nondestructive testing of new technology, and new sensor technology.

(Executive Editor: Xu Chengting)